Semiconducting SWNTs sorted by polymer wrapping

Derenskyi, Vladimir; Gomulya, Widianta; Gao, Jia; Bisri, Satria Zulkarnaen; Pasini, Mariacecilia; Loo, Yueh-Lin; Loi, Maria Antonietta

Published in:
Journal of Materials Research

DOI:
10.1063/1.5011388

Publication date:
2018

Semiconducting SWNTs sorted by polymer wrapping: How pure are they?

Vladimir Derenskyi, Widianta Gomulya, Jia Gao, Satria Zulkarnaen Bisri, Mariacecilia Pasini, Yueh-Lin Loo, and Maria Antonietta Loi

Citation: Appl. Phys. Lett. **112**, 072106 (2018); doi: 10.1063/1.5011388

View online: https://doi.org/10.1063/1.5011388

View Table of Contents: http://aip.scitation.org/toc/apl/112/7

Published by the American Institute of Physics

Semiconducting SWNTs sorted by polymer wrapping: How pure are they?

Vladimir Derenskyi,[1] Widianta Gomulya,[1,2] Jia Gao,[3] Satria Zulkarnaen Bisri,[1,2] Mariacecilia Pasini,[4] Yueh-Lin Loo,[3,5] and Maria Antonietta Loi[1,a)]
[1]*Zernike Institute for Advanced Materials, University of Groningen, Nijenborgh 4, Groningen 9747 AG, The Netherlands*
[2]*RIKEN Center for Emergent Matter Science (CEMS), 2-1 Hirosawa, Wako-shi, Saitama 351-0198, Japan*
[3]*Department of Chemical and Biological Engineering, Princeton University, Princeton, New Jersey 08544, USA*
[4]*Istituto per lo Studio delle Macromolecole (CNR), Via A. Corti 12, 20133 Milano, Italy*
[5]*Andlinger Center for Energy and the Environment, Princeton University, Princeton, New Jersey 08544, USA*

(Received 31 October 2017; accepted 5 February 2018; published online 16 February 2018)

Short-channel field-effect transistors (FETs) prepared from semiconducting single-walled carbon nanotube (s-SWNT) dispersions sorted with poly(2,5-dimethylidynenitrilo-3,4-didodecylthienylene) are demonstrated. Electrical analysis of the FETs shows no evidence of metallic tubes out of a total number of 646 SWNTs tested, implying an estimated purity of our semiconducting SWNT solution higher than 99.85%. These findings confirm the effectiveness of the polymer-wrapping technique in selecting semiconducting SWNTs, as well as the potential of sorted nanotubes for the fabrication of short channel FETs comprising from 1 to up to 15 nanotubes without inter-nanotube junctions. *Published by AIP Publishing.* https://doi.org/10.1063/1.5011388

Single-walled carbon nanotubes (SWNTs) remain one of the strongest candidates for the applications of high-performance nanoscale field-effect transistors (FETs). The one-dimensional nature of SWNTs and properties such as intrinsic ambipolarity,[1] high carrier mobility,[2] and ballistic electron transport[3] make them perfect building blocks for the fabrication of transistors for high-speed, low-cost, and low power-consumption electronics. In order to utilize the full potential of SWNTs in FETs, however, a few challenges must be overcome, including the separation of metallic (m-SWNT) and semiconducting (s-SWNT) species present in the as-synthesized material. After a decade of extensive research in the field of sorting s-SWNTs, post-growth purification techniques, such as column chromatography,[4] dielectrophoresis,[5] density gradient ultracentrifugation,[6,7] weak field centrifugation,[8] and DNA[9] and polymer-assisted SWNT separation,[10] have been successfully developed.

One of the most promising techniques for sorting s-SWNTs is the one using conjugated polymers, which takes the advantage of the non-covalent interaction of the backbone and side chains of certain conjugated polymers with SWNTs with specific structures.[10] This method has significant advantages over other techniques, including the high purity of the sorted s-SWNTs, minimal detrimental effect on their structure, ease of processing and high reproducibility and scalability.[11]

Following the discovery of this method, polyfluorene-[12] and polythiophene-based[13] conjugated polymers with different side-chains[14] have demonstrated excellent ability to select semiconducting SWNTs based on their helicity and/or diameters. Indeed, s-SWNT dispersions prepared in this way have enabled the fabrication of high-performance SWNT network-based FETs exhibiting high on/off current ratio modulation (up to 10^8)[15] and charge mobility above 30 $cm^2/V{\cdot}s$.[14,16] A trade-off between the extracted field-effect mobility and the current on/off ratio is generally observed, which has been ascribed to the presence of residual metallic nanotubes in the carbon nanotube networks that work as FET channels. Due to the fact that most FETs reported so far comprise a device channel much longer than the average length of the dispersed carbon nanotube, the FETs may still exhibit high current on/off ratios when the metallic species are below the percolation threshold.[17]

Such an observation casts doubts on the actual purity of polymer-sorted s-SWNTs, even though spectroscopic characterization shows no detectable signals of m-SWNTs. For the ultimate goal of building a nanoscale logic circuit with s-SWNTs, a reliable evaluation of the semiconductor purity of polymer-wrapped SWNTs is desirable.

Statistical analysis of the electrical performance of single-nanotube field-effect transistors is a more reliable approach to evaluate the purity of s-SWNT dispersion compared to spectroscopic methods. Recently, single-tube transistors based on s-SWNT dispersions prepared using either column chromatography[18] or polymer sorting[19] have been demonstrated. In the polymer sorting work, the purity of semiconducting SWNT solutions sorted with polyfluorene was estimated by evaluating the on/off ratios of transistors having a channel length of 240 nm using arrays of SWNTs.[19]

Recently, we reported the high yield (16%) sorting of semiconducting SWNT by using the polymer poly(2,5-dimethylidynenitrilo-3,4-didodecylthienylene) (PAMDD).[16] Field-effect transistors comprising such carbon nanotube networks exhibit mobilities above 30 cm^2/V s and an on/off ratio of 10^6.

In this article, we report the performance of field-effect transistors comprising individual PAMDD-wrapped s-SWNT as the active channel. Field-effect transistors with a channel length of 300 nm, i.e., smaller than the average length of the SWNTs, were fabricated. On/off current ratios as high as 10^5 for electron enhancement and 10^4 for hole enhancement regimes were obtained. The distribution of the on current and

a)E-mail: m.a.loi@rug.nl

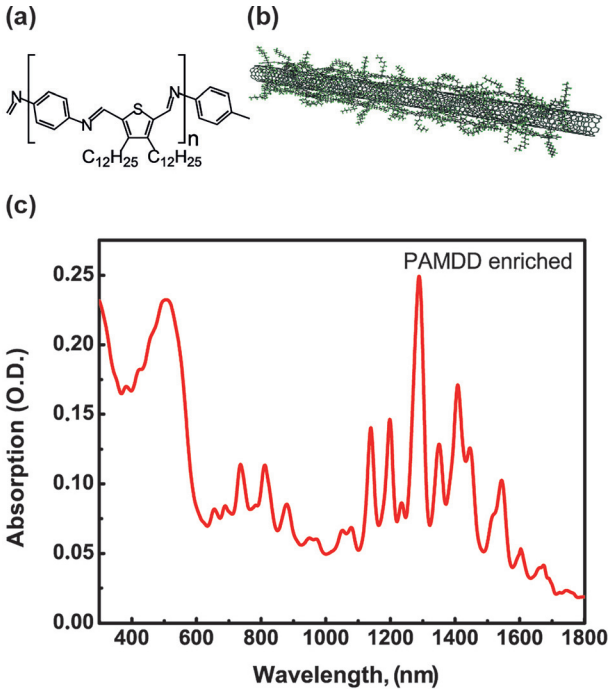

FIG. 1. (a) Chemical structure of the PAMDD polymer used for the selection of the semiconducting SWNTs, (b) schematic structure of a SWNT wrapped by polymer chains, and (c) absorption spectra of the enriched HiPCO-PAMDD nanotube solution.

the threshold voltages displays high stability over 190 fabricated devices. Moreover, in none of the measured devices, a short-circuit was observed. Such a short-circuit would occur in short-channel SWNT-based FETs only if metallic SWNT species would be present in the channel. Given the absence of short-circuited devices, the statistical results indicate that the PAMDD-sorted s-SWNT dispersion contains >99.85% pure semiconducting species.

s-SWNTs were selected with a polyazomethine (PAMDD)[16,20–22] polymer. The chemical structure of PAMDD is shown in Fig. 1(a). The polymer was synthesized through a condensation reaction between 2,5-Diformyl-3,4-didodecylthiophene and *p*-phenylenediamine. It is worthy to note that imine polymerization does not require any metal catalysts typically used for traditional conjugated polymer synthesis. Moreover, imine chemistry seems to be very promising for the development of "green electronics" thanks to the absence of noble metal catalysts and toxic phosphorous ligands, which allows a totally disintegrable and biocompatible semiconducting polymer.[23]

The selection process (see supplementary material) consists of two main steps, ultrasonication and ultracentrifugation.[24] Briefly, the ultrasonication process destroys nanotube bundles, allowing the polymer to interact with the walls of SWNTs [Fig. 1(b)] and to disperse individual nanotubes in organic solvents. During ultracentrifugation, the undispersed metallic nanotubes, bundles, and other forms of carbon present in the as-synthesized material precipitate are then removed. The excellent s-SWNT extraction yield (16%) obtained with PAMDD is attributed to the presence of nitrogen atoms in the polymeric backbone, which display a very high affinity for the polarizable walls of SWNTs; the details on this mechanism and attribution of chirality and diameter of the SWNTs extracted have been reported elsewhere.[16]

The absorption spectrum of the HiPCO-PAMDD solution is shown in Fig. 1(c). Two sets of sharp peaks in the ranges between 600 nm–900 nm and 1000 nm–1600 nm corresponding to the second (S_{22}) and the first (S_{11}) electronic transitions of s-SWNTs, respectively, are observed. The first electronic transitions of metallic nanotubes, M_{11}, usually appear in the range between 400 nm and 600 nm. However, the broad absorption peak of PAMDD in the same range masks any signature of metallic nanotubes, even if they were present. This spectral overlap thus precludes the quantification of the purity of s-SWNTs by absorption spectroscopy.

Even though FETs with high mobility and a current on/off ratio based on this dispersion have been demonstrated,[16] we did not previously quantify the purity of semiconducting SWNTs. Being the extraction yield of this polymer one of the highest is important to quantify the number of metallic tubes, as very often, the effectiveness in selecting semiconducting tubes is inversely proportional to the yield. Herein, we then adopt an alternative method of evaluating the purity of s-SWNTs in the HiPCO-PAMDD solution by analyzing the charge-transport characteristics of the short-channel FETs, i.e., of devices with the source-drain distance shorter than the average length of s-SWNTs (approx.1 μm).[24]

Figure 2(a) shows the optical micrograph of the fabricated devices with a central source electrode and 12 surrounding drain electrodes. The channel region of one such device is illustrated in Fig. 2(b). The channel length is as short as 300 nm; this length was chosen to avoid the formation of a

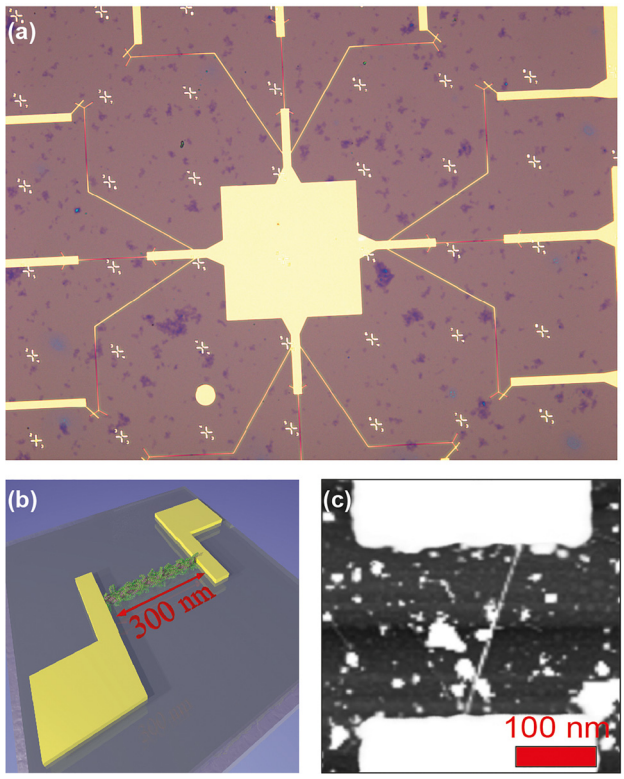

FIG. 2. (a) Optical image of the fabricated FETs; one substrate includes 12 FETs with the common source electrode in the center and drain electrodes at the edges. (b) Schematic structure of the single SWNT device. (c) Atomic force microscopy (AFM) image of the source and drain electrodes forming the FET channel together with an individual SWNT. The channel width and length are 300 nm.

SWNT network with nanotube-nanotube junctions within the transistor channel. In addition, the 300-nm channel width minimizes the probability of multiple SWNTs assembled in the channel region. Using this configuration, we were able to study the performance of devices based on single or few s-SWNT bridging the source and drain electrodes.

Two sets of SWNT FETs were fabricated for this experiment. HiPCO-PAMDD solutions with different s-SWNT concentrations were spin-coated on top of highly doped Si wafer with thermally grown SiO_2. The top Ti/Au source and drain electrodes were subsequently defined by electron-beam lithography (Raith e-Line with a spatial resolution of 6 nm). The experiment was repeated three times for each solution concentration for a total of 150 and 40 fabricated devices with the low and the high concentration solutions, respectively. Figure 2(c) displays the atomic force microscopy (AFM) (see for details the supplementary material) micrograph of a FET with an individual PAMDD-wrapped s-SWNT deposited between the electrodes; this sample was obtained with the low concentration solution. The white spots on the image are most probably due to residual PAMDD from the selection process and/or from incomplete removal of photoresist during the lithographic step.

The drain (V_D) and the gate (V_G) voltage dependences of the drain current are shown in Figs. 3(a) and 3(b), respectively. Of 150 s-SWNT transistors measured, 46 exhibited semiconducting behavior and 104 FETs showed no drain current, due to the absence of nanotubes between the electrodes. This was verified by performing detailed AFM imaging in the channels of these devices. The relatively low yield of functional devices (31%) is primarily due to the low probability of matching the randomly distributed SWNTs on the substrate with the top electrodes.

Because of the bottom-gate structure with conventional SiO_2 as a gate dielectric, the devices were operated up to 60 V. Figure 3(a) shows the $I_D - V_D$ output characteristic of a single SWNT device; due to short-channel effects and the presence of contact resistance, the output characteristics do not saturate as one would have predicted. The devices are ambipolar with the maximum hole current of about 0.2 μA and electron current around 25 nA. The transconductance curves showing values up to 8 nS are reported in the inset of Fig. 3(c). These values are comparable with previously reported results on FETs made with a few polymer-wrapped SWNTs per channel,[25] but because of the SiO_2 gate dielectric, they do not compete with the best devices reported recently using poly[(9,9-dioctylfluorenyl-2,7-diyl)-alt-co-(6,60–(2,20-bipyridine))] (PFO-BPy) wrapped SWNTs.[26] The current in the *off*-state [Fig. 3(b)] was as low as 5 pA and was limited by the resolution of the measurement set-up. The measured *on*- and *off*-currents in working transistors resulted in an average on/off ratio of 10^5 [Fig. 3(b)]. Despite being limited by the applied drain voltage, these on/off ratio values are very high and comparable with the highest reported on/off ratios for solution-processed SWNT FETs with short transistor channels.[25]

Unlike previous reports,[27] showing that SWNT FETs with Ti/Au electrodes usually display unipolar p-type characteristics when fabricated in ambient conditions due to the trapping of electrons by adsorbed oxygen molecules,[28] our devices show ambipolar electrical behavior even though the device fabrication was also performed in ambient conditions. This recovery in ambipolarity likely stems from post-deposition annealing of the transistors, carried out at 200 °C in the nitrogen atmosphere for 2 h, which allows the desorption of oxygen and water molecules[29–31] and reestablishes the intrinsic charge transport properties.

To further understand the uniformity of the electrical properties of PAMDD-sorted s-SWNTs, we fabricated devices starting from a more concentrated solution. Figure 4(a) shows

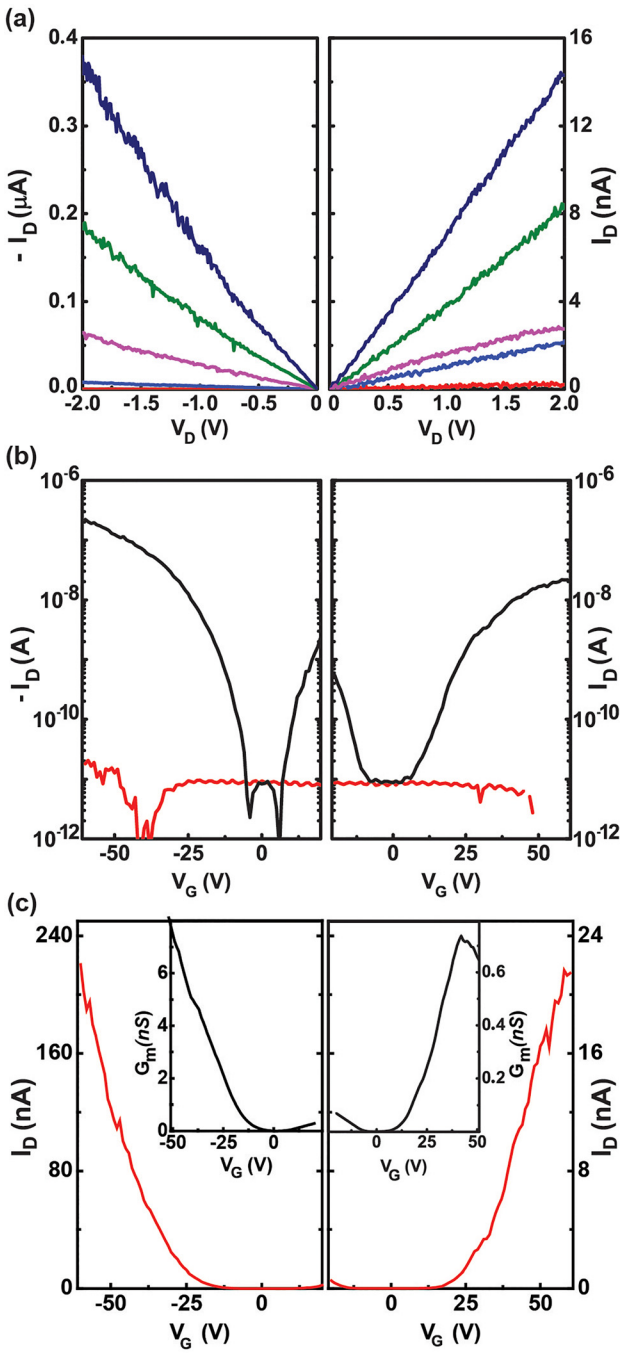

FIG. 3. Electrical measurements of a single SWNT FET. (a) Output $I_D - V_D$ demonstrates the gate-effect for V_D varying between 0 and 50 V (−50 V) with steps of 10 V (−10 V). (b) Transfer $I_D - V_G$ characteristics for p- and n-type channels measured in the linear operational regime at $|V_D| = 0.4$ V. Drain current (I_D, black curve) and Gate current (I_G, red curve) (c) transfer $I_D - V_G$ characteristics on the linear scale. Insets: Transconductance plot for single SWNT FET.

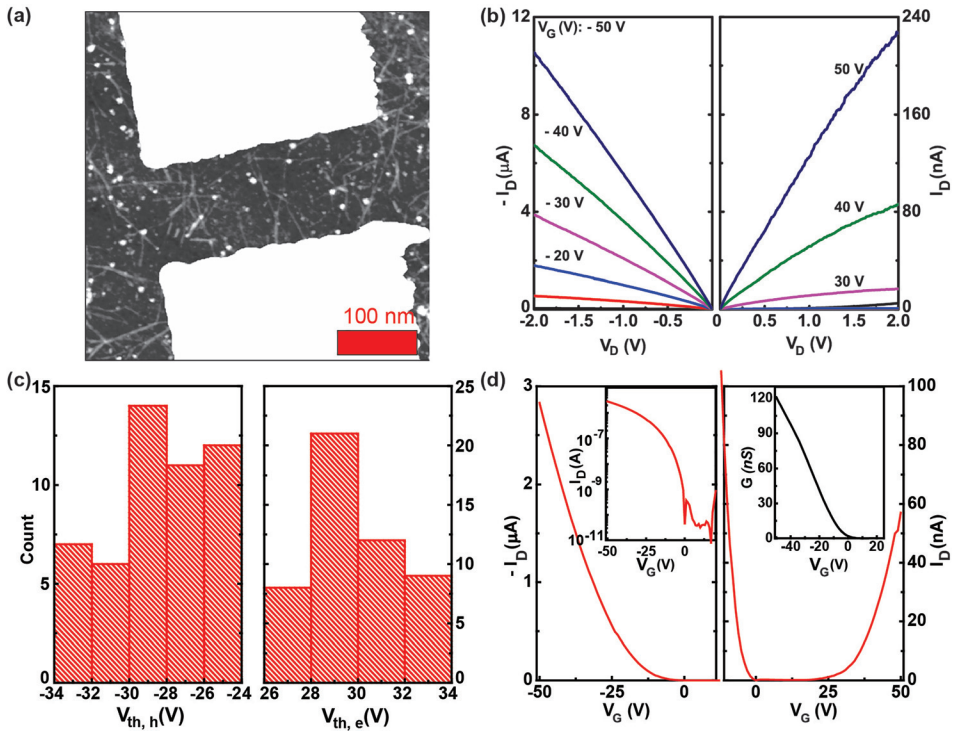

FIG. 4. (a) AFM image of the channel region. (b) Output characteristics ($|V_D| = 0.4$ V) of FETs with few SWNTs crossing the channel. Hole current in this FET demonstrates a 25 times increase compared to that in a single SWNT FET. (c) Statistics of the threshold voltages for hole and electron currents. (d) Linear scale of the transfer $I_D - V_G$ characteristics for p- and n-type channels measured at $|V_D| = 0.4$ V. Insets: Transfer characteristic in the hole-only regime on the logarithmic scale (left) and transconductance in the hole only regime plot for multiple SWNT FET (right).

an AFM micrograph showing one of these transistors with several SWNTs between the electrodes. Figures 4(b) and 4(d) display representative $I_D - V_D$ (output) and $I_D - V_G$ (transfer) characteristics, respectively, obtained in a device comprising 10–15 s-SWNTs. The transistors show higher hole current, about 12 μA at $V_G = -50$ V and $V_D = -2$ V, and the electron current (for $V_G = 50$ V and $V_D = 2$ V) is about 200 nA compared to those based on individual nanotubes (shown in Fig. 3). The current appears to scale approximately with the number of s-SWNTs bridging the channel, indicating that each nanotube, regardless of chirality (few chiralities are present in the starting solution [see Fig. 1(c)], carries similar current under the same conditions. Such uniformity is desirable for the integration of SWNT-based FETs into arrays and circuits. Figure 4(c) also shows the stability of the threshold shift over all the single nanotube devices.

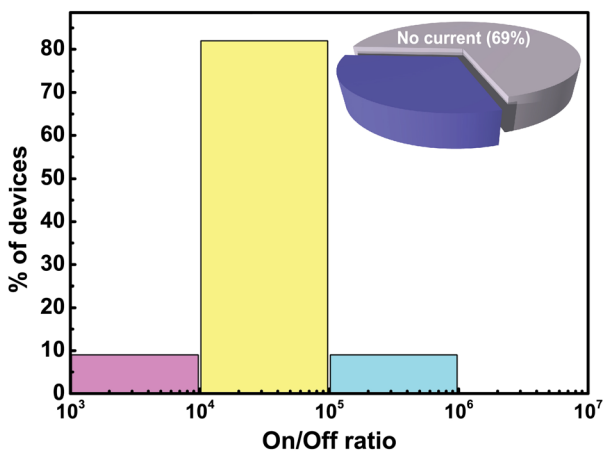

FIG. 5. Diagram representing the distribution of the on/off ratio in 150 FETs measured with single SWNT in the channel region. 69% of fabricated devices did not show any current due to the absence of SWNTs in channels. Working FETs demonstrated an average on/off current ratio of 10^5.

Figure 4(d) shows the transfer characteristics in the linear regime. That the current on/off ratio values reaches more than 10^5 proves that all tubes within the channels are semiconducting. The inset of Fig. 4(d) shows the conductance of the same device.

The diagram reported in Fig. 5 presents the statistical distribution of the on/off ratio of the fabricated transistors. 80% of working devices demonstrate an average on/off current ratio of 10^5 and only about 9% show on/off between 10^4 and 10^3. Interestingly, of the 150 devices with single nanotubes and of the 40 devices with multiple tubes (an average of 15 tubes per device), for a total of 646 SWNTs measured, none of them failed short circuit. Therefore, from these data, we can estimate that the percentage of metallic tubes in our samples is lower than 0.15%, corresponding to a purity of semiconducting carbon nanotube solution >99.85%. This value is an underestimate; since no short-circuits were detected, to precisely determine the purity of this high quality sample, a much larger number of devices would be required to precisely determine the purity of our s-SWNTs.

We have demonstrated statistical analysis on single-SWNT FETs prepared from PAMDD-wrapped s-SWNT solutions. Of 46 working single s-SWNT FETs and 40 multiple tube (avg. 15 tubes) FETs, an average on/off current ratio of 10^5 is observed. No traces of metallic SWNTs were found in any of the prepared FETs (646 SWNTs tested), indicating an estimated purity of our semiconducting SWNT solution higher than 99.85%. Statistical analysis of the electrical conductance of s-SWNTs and of the threshold voltage (15% variation) of SWNT-based FETs suggests rather uniform electrical characteristics of dispersed s-SWNT. These findings confirm the effectiveness of the PAMDD in selecting semiconducting SWNTs, as well as the potential of the sorted nanotubes for short-channel FET application.

See supplementary material for the detailed experimental section.

The technical support of Arjen Kamp and Johan Holstein is acknowledged. The Groningen team would like to thank the Stichting voor de Technische Wetenschappen (STW, Utrecht, the Netherlands) for financial support. We would also like to thank Mario Caironi for discussions.

[1]S. Z. Bisri, C. Piliego, J. Gao, and M. A. Loi, Adv. Mater. **26**, 1176 (2014).
[2]T. Dürkop, S. A. Getty, E. Cobas, and M. S. Fuhrer, Nano Lett. **4**, 35 (2004).
[3]A. Javey, J. Guo, Q. Wang, M. Lundstrom, and H. Dai, Nature **424**, 654 (2003).
[4]H. Liu, D. Nishide, T. Tanaka, and H. Kataura, Nat. Commun. **2**, 309 (2011).
[5]R. Krupke, F. Hennrich, H. V. Löhneysen, and M. M. Kappes, Science **301**, 344 (2003).
[6]M. S. Arnold, S. I. Stupp, and M. C. Hersam, Nano Lett. **5**, 713 (2005).
[7]M. S. Arnold, A. A. Green, J. F. Hulvat, S. I. Stupp, and M. C. Hersam, Nat. Nanotechnol. **1**, 60 (2006).
[8]W. G. Reis, R. T. Weitz, M. Kettner, A. Kraus, M. G. Schwab, Ž. Tomović, R. Krupke, and J. Mikhael, Sci. Rep. **6**, 26259 (2016).
[9]M. Zheng, A. Jagota, E. D. Semke, B. A. Diner, R. S. Mclean, S. R. Lustig, R. E. Richardson, and N. G. Tassi, Nat. Mater. **2**, 338 (2003).
[10]A. Nish, J.-Y. Hwang, J. Doig, and R. J. Nicholas, Nat. Nanotechnol. **2**, 640 (2007).
[11]S. K. Samanta, M. Fritsch, U. Scherf, W. Gomulya, S. Z. Bisri, and M. A. Loi, Acc. Chem. Res. **47**, 2446 (2014).
[12]W. Gomulya, G. D. Costanzo, E. J. F. de Carvalho, S. Z. Bisri, V. Derenskyi, M. Fritsch, N. Fröhlich, S. Allard, P. Gordiichuk, A. Herrmann, S. J. Marrink, M. C. dos Santos, U. Scherf, and M. A. Loi, Adv. Mater. **25**, 2948 (2013).
[13]H. W. Lee, Y. Yoon, S. Park, J. H. Oh, S. Hong, L. S. Liyanage, H. Wang, S. Morishita, N. Patil, Y. J. Park, J. J. Park, A. Spakowitz, G. Galli, F. Gygi, P. H.-S. Wong, J. B.-H. Tok, J. M. Kim, and Z. Bao, Nat. Commun. **2**, 541 (2011).
[14]S. P. Schießl, N. Fröhlich, M. Held, F. Gannott, M. Schweiger, M. Forster, U. Scherf, and J. Zaumseil, ACS Appl. Mater. Interfaces **7**, 682 (2015).
[15]V. Derenskyi, W. Gomulya, J. M. Salazar-Rios, M. Fritsch, N. Fröhlich, S. Jung, S. Allard, S. Z. Bisri, P. Gordiichuk, A. Herrmann, U. Scherf, and M. A. Loi, Adv. Mater. **26**, 5969 (2014).
[16]W. Gomulya, V. Derenskyi, E. Kozma, M. Pasini, and M. A. Loi, Adv. Funct. Mater. **25**, 5858 (2015).
[17]C. Wang, J. Zhang, K. Ryu, A. Badmaev, L. G. De Arco, and C. Zhou, Nano Lett. **9**, 4285 (2009).
[18]G. S. Tulevski, A. D. Franklin, and A. Afzali, ACS Nano **7**, 2971 (2013).
[19]G. J. Brady, Y. Joo, M.-Y. Wu, M. J. Shea, P. Gopalan, and M. S. Arnold, ACS Nano **8**, 11614 (2014).
[20]S. Destri, M. Pasini, C. Pelizzi, W. Porzio, G. Predieri, and C. Vignali, Macromolecules **32**, 353 (1999).
[21]T. Lei, X. Chen, G. Pitner, H.-S. P. Wong, and Z. Bao, J. Am. Chem. Soc. **138**, 802 (2016).
[22]T. Lei, I. Pochorovski, and Z. Bao, Acc. Chem. Res. **50**, 1096 (2017).
[23]T. Lei, M. Guan, J. Liu, H. C. Lin, R. Pfattner, L. Shaw, A. F. McGuire, T.-C. Huang, L. Shao, K.-T. Cheng, J. B. H. Tok, and Z. Bao, Proc. Natl. Acad. Sci. **114**, 5107 (2017).
[24]S. Z. Bisri, J. Gao, V. Derenskyi, W. Gomulya, I. Iezhokin, P. Gordiichuk, A. Herrmann, and M. A. Loi, Adv. Mater. **24**, 6147 (2012).
[25]S. Park, H. W. Lee, H. Wang, S. Selvarasah, M. R. Dokmeci, Y. J. Park, S. N. Cha, J. M. Kim, and Z. Bao, ACS Nano **6**, 2487 (2012).
[26]G. J. Brady, A. J. Way, N. S. Safron, H. T. Evensen, P. Gopalan, and M. S. Arnold, Sci. Adv. **2**, e1601240 (2016).
[27]A. Javey, H. Kim, M. Brink, Q. Wang, A. Ural, J. Guo, P. McIntyre, P. McEuen, M. Lundstrom, and H. Dai, Nat. Mater. **1**, 241 (2002).
[28]V. Derycke, R. Martel, J. Appenzeller, and P. Avouris, Appl. Phys. Lett. **80**, 2773 (2002).
[29]A. Javey, J. Guo, D. B. Farmer, Q. Wang, E. Yenilmez, R. G. Gordon, M. Lundstrom, and H. Dai, Nano Lett. **4**, 1319 (2004).
[30]S. J. Wind, J. Appenzeller, R. Martel, V. Derycke, and P. Avouris, Appl. Phys. Lett. **80**, 3817 (2002).
[31]R. V. Seidel, A. P. Graham, J. Kretz, B. Rajasekharan, G. S. Duesberg, M. Liebau, E. Unger, F. Kreupl, and W. Hoenlein, Nano Lett. **5**, 147 (2005).